Technical Report: Supplemental Simulation and Experimental Results for Cog-TV

Zhongyuan Zhao, *Member, IEEE*, Mehmet C. Vuran, *Member, IEEE*, Demet Batur, and Eylem Ekici, *Fellow, IEEE*

1 Introduction

In this technical report, additional simulation and experimental evaluations of the technical framework, Cognitive Television (Cog-TV), are presented to support the feasibility and potential of TV receiver-assisted unlicensed spectrum access. The technical framework of Cog-TV is first proposed in [1], and a prototype is developed in [2], more detailed analysis and modeling are included in [3]. The content of this report is organized as follows: The impact of market penetration rate on spectrum availability is presented in Section 5, Optimization of the size of interference zone is presented in Section 6, complementary materials in site survey are reported in Section 7, city-wide evaluation supplementals are reported in Section 8, and the catagorized spectrum and capacity results are reported in 9.

2 Gray Space Population Density Requirement

Gray space is defined as spatio-spectral space where OTA TV service is active but TV receiver is absent. Consider the guard zone around a TV receiver has a radius of $R_{tv} = 910m$ [4], and the TV receiver location follows homogeneous Poisson Point Process with density $\lambda = \rho\eta$, where ρ is population density, and $\eta = 13.3\%$ is the OTA TV ownership rate. The gray space is considered unavailable in the interested region, if the distance between an arbitrary secondary user and its nearest TV receiver is equal to or smaller than R_{tv} with a probability greater than a constant, p. Based on the Nearest Neighbor Function in 2D plane, $D(R_{tv}) = 1 - \exp(-\lambda\pi R_{tv}^2)$, we can find the critical population density for gray space given p, is $\rho(p) = \frac{\ln(1-p)}{-\pi R_{tv}^2 \eta}$, e.g. $\rho(0.95) = 8.65/km^2$, $\rho(0.84) = 5.3/km^2$, and $\rho(0.80) = 4.65/km^2$. For example, $\rho(0.95) = 8.65/km^2$ stands for the probability of an arbitrary secondary user falls in the guard zone of a TV receiver in the region with a population density of $8.65/km^2$ is 95%.

- *Zhongyuan Zhao and Mehmet C. Vuran are with the Department of Computer Science and Engineering, University of Nebraska-Lincoln, Lincoln, Nebraska 68588, USA (e-mail: {zhzhao;mcvuran}@cse.unl.edu)*
- *Demet Batur is with the Department of Management, University of Nebraska-Lincoln, Lincoln, Nebraska 68588, USA (e-mail:dbatur@unl.edu)*
- *Eylem Ekici is with the Department of Electrical and Computer Engineering, The Ohio State University, Columbus, Ohio 43210, USA (e-mail: ekici@ece.osu.edu)*

A preliminary version of this paper has appeared on Globecom 2014 [1]. This work is supported by NSF under grant number CNS-1247941 and CNS-1247914.

3 K-Peicewise Zipf Model

In a K-Piecewise Zipf model, the SHR of channel b_j is expressed as:

$$r(b_j) = Z(k(b_j)) = a_i k(b_j)^{-\tau_i}, k(b_j) \in \left(k'_{i-1}, k'_i\right] \text{ for } i = 1, \ldots, K \ , \tag{1}$$

where $k(b_j)$ is the rank of channel b_j by SHR in a descending order, the K pieces are defined by change points $k'_0, \ldots, k'_K$, where $k'_0 = 0, k'_K = |\mathbb{T}|$, and $k'_{i-1} < k'_i, \forall i \in \{[1, K]\}$, and the parameters $\tau_i > 0$, $a_i > 0$ are constrained by normalization. Estimation of parameters and change points can be found in [5] and [6], respectively. The rank vector is modeled as a random permutation of $\langle 1, \ldots, |\mathbb{T}|\rangle$:

$$\mathbf{k} = \left\langle k(b_1), \ldots, k(b_j), \ldots, k(b_{|\mathbb{T}|})\right\rangle \in \mathbf{Sym}(\{[1, |\mathbb{T}|]\}) \ , \tag{2}$$

where $\mathbf{Sym}(.)$ denotes the symmetric group on a set.

4 Distribution of $V_{\Delta,z,t}(\mathbf{k})$

Based on Combinatorial Central Limit Theorem [7], when $\mathbf{k}$ is a random permutation of $\langle 1, \ldots, |\mathbb{T}|\rangle$, $V_{\Delta,z,t}(\mathbf{k})$ in (**??**) follows a Normal distribution with mean and variance as:

$$E(V_{\Delta,z,t}(\mathbf{k})) = \frac{|\mathbb{B}|}{|\mathbb{T}|} \sum_{i=1}^{|\mathbb{T}|} U(i) \ , \tag{3}$$

$$Var(V_{\Delta,z,t}(\mathbf{k})) = \frac{1}{|\mathbb{T}|} \sum_{b_j \in \mathbb{T}} \sum_{i=1}^{|\mathbb{T}|} D^2\left(b_j, i\right) \ , \tag{4}$$

respectively, where, with $\mathbb{I}(.)$ as indicator function, $D(b_j, i)$ is defined as:

$$\begin{aligned} D(b_j, i) = \mathbb{I}(b_j \in \mathbb{B}) &\left(U(i) - \frac{1}{|\mathbb{T}|} \sum_{n=1}^{|\mathbb{T}|} U(n)\right) \\ &+ \frac{|\mathbb{B}|}{|\mathbb{T}|} \left(\sum_{n=1}^{|\mathbb{T}|} U(n) - U(i)\right) \ . \end{aligned} \tag{5}$$

5 Market Penetration Ratio

With a cell size of $R = 150m$, the average black-space spectrum availability (SA) by market penetration rate in 6 U.S. cities are illustrated in Fig. 1. It can be observed that for cities with low population density, such as, Lincoln, NE, SA could be high at even lower market penetration rate. However, for cities with high

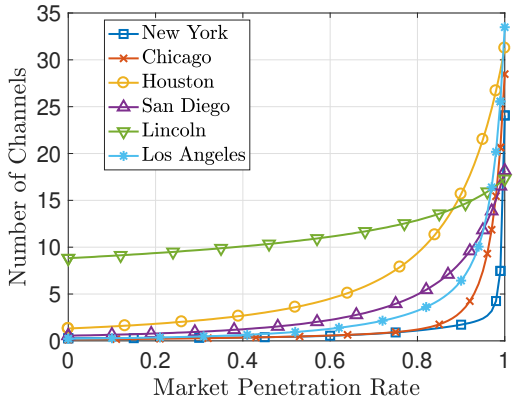

Fig. 1. Average Black-Space Spectrum Availability v.s Market Penetration Rate in 6 Cities, $R = 150m$.

population density, such as New York City, Chicago, it will require a very high market penetration rate to enable most of the SA in black-space. This is because the chance of having a traditional TV receiver in a Cog-TV cell increases by population density for a certain market penetration rate.

6 Optimal Interference Radius

The radius of service zone, d, in Cog-TV cell is application specific, thus generally not adjustable. The interference radius, R, however, could determine the achievable capacity of Cog-TV cell. Larger R would allow higher transmit power and hence, higher session capacity, but reduce SA by including more PUs in its interference region. Since our model is based on statistical models of many environmental factors, we aim to find an optimal cognitive range for each market (i.e. an metropolitan area, a city, sub-region of a city). For example, Cog-TV cell size optimization for city y is

$$R^* = \underset{R}{\operatorname{argmax}}\, E\Big(C_t^b(R)\Big)\ . \tag{6}$$

The average achievable capacity as a function of cognitive range in 6 U.S. cities, with both PU and SU outdoor, are illustrated in Fig. 2.

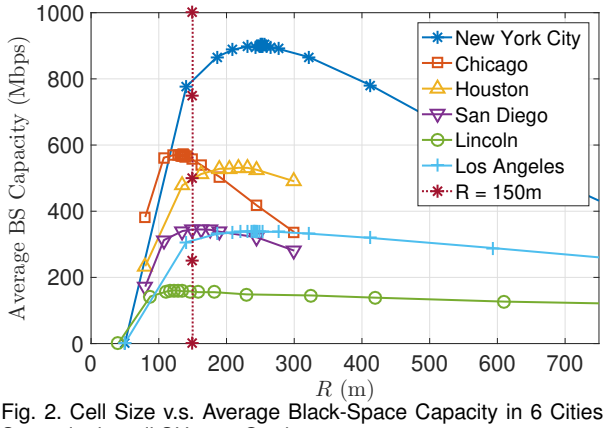

Fig. 2. Cell Size v.s. Average Black-Space Capacity in 6 Cities for the Scenario that all SUs are Outdoor, $d = 10m$.

However, the optimal cognitive range obtained from (6) only applies for a simple scenario, i.e. specific TV ratings, single antenna in SU transceiver, certain radio propagation scenario. Moreover, the SA may outweigh the total capacity for some wireless networks. For more realistic yet complex scenarios, e.g. SU equipped multiple antennas, mixed indoor and outdoor environments, and temporal variations of TV viewership over a day, the optimal cognitive range could be the weighted average of the R^* for multiple simple scenarios. Thus, more practical optimization is out of the scope of this paper. Nevertheless, we use $R = 150m$ in the following evaluations as it yield fairly good performance in all the cities.

7 Site Survey for Cog-TV Power Control

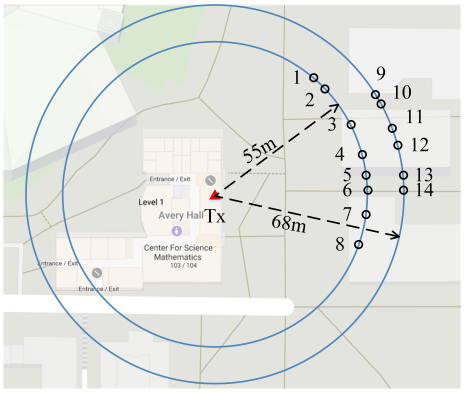

(a)

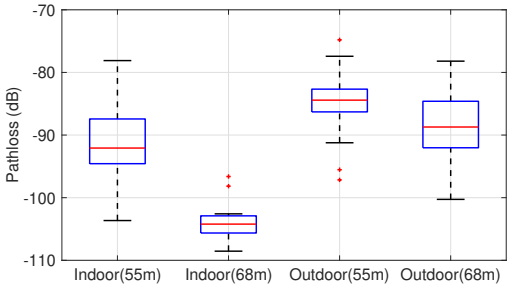

(b)

Fig. 3. Indoor–Indoor and Indoor–Outdoor Channel Gain Measurement: (a) Experiment Site, (b) Measured Channel Gain.

An experiment for testing the indoor to indoor interference between co-channel secondary users are conducted on campus site. The placement of transmitter and receivers are illustrated in Fig. 3(a). The transmiter is placed indoor on the ground floor of a building, and receivers are located indoors in another building and outdoors, at distances of $55m$ to $68m$ from the transmitter. The channel gains from indoor SU transmitter to SU receivers at indoors and outdoors at $55m$ and $68m$ are illustrated in Fig. 3(b). Indoor SUs is less interfered than outdoor SUs by co-channel SU transmitter, due to the shielding of buildings. Moreover, the interference from indoor to indoor is attenuated faster than from indoor to outdoor, since more obstacles (walls) on the path. Since the majority of SU of WLAN would be located indoor, they would experience much less co-channel interference than at outdoors.

In Figs. 4, we repeated aforementioned analysis in Section V-II of [3] but with site specific pathloss model obtained from measurement data. The protection of TV receivers are the same as in [3], but it can be observed that with a more accurate pathloss, higher SU transmit power could be employed to improve the SU SINR without causing interference to PU. In practice, network operators may optimize path loss model in their deployment based on spectrum sensing.

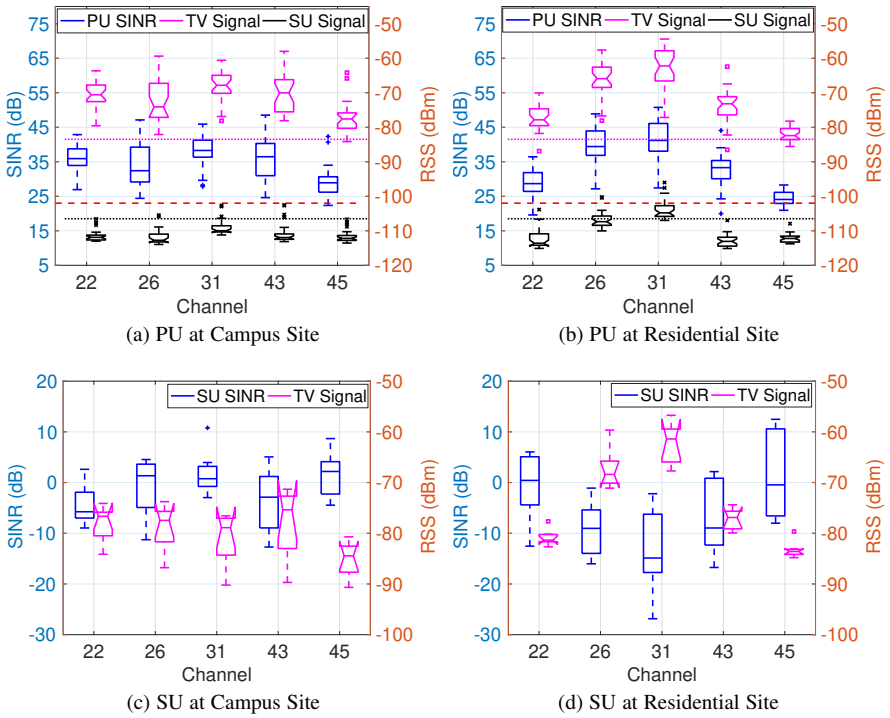

(a) PU at Campus Site (b) PU at Residential Site

(c) SU at Campus Site (d) SU at Residential Site

Fig. 4. Measured SINR of SU and PU at Campus and Residential Sites with Site specific pathloss model.

8 City Wide Evaluation on Achievable Capacity

The heat maps of population density by Zip-code district of the evaluated cities: New York City and Lincoln are illustrated in Figs. 5.

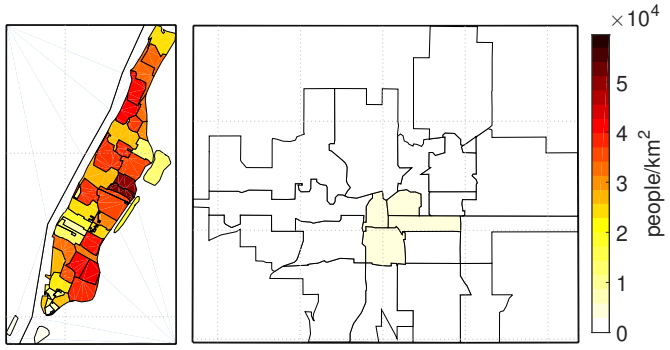

(a) New York City (b) Lincoln, Nebraska

Fig. 5. CENSUS 2010 Population Density by ZIP code.

8.1 Spectrum Availability

The CDFs of Black Space Spectrum Availability in New York City, with Zipf SHR in [**?**], OTA TV Ownership $\eta = 38\%$, and HUT 60%, from city-level spectrum availability model, and grid-by-grid simulation and cellular model are illustrated in Fig. 6. Even in this hypothetical TV ownership rate where all OTA services carried in cable, satelites, Internet, and etc. are served by broadcast only, there are still 20 OTA TV channels available in New York City.

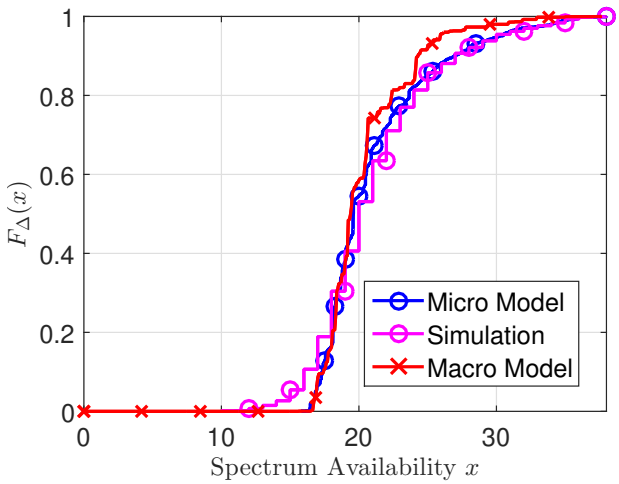

Fig. 6. CDFs of Black Space Spectrum Availability in New York City, Zipf SHR, OTA TV Ownership $\eta = 38\%$, HUT 60%. 38% include all the TV viewers watching the programs of broadcast TV networks in the US screamed by not only OTA TV service but all kinds of sources according to Nielsen Rating.

8.2 Achievable Capacity

With a single antenna without interference cancellation technology, the session capacity of secondary user in TV black-space with Cog-TV transmit power control are significantly lower than capacity in TV white-space even under the same level of TV signal interference, as shown in Figs. 7(a) and 7(b), resp. This is because of the need of protecting TV receivers would significantly limit the transmit power of SU, while there is no TV receivers in TV white space. Under strong primary interference, session capacity on white and black space channels are both low as the ERP is limited by regulation, e.g. 16dBm. As the primary interference

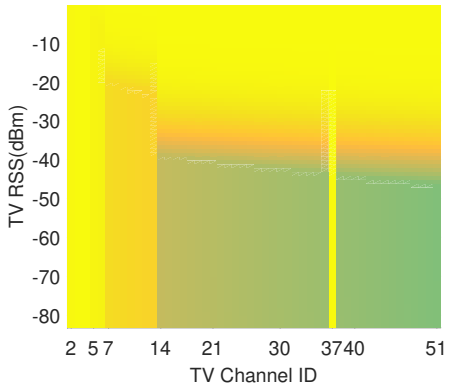

(a) Black Space

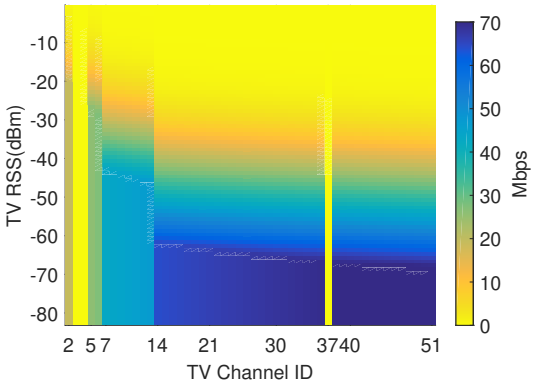

(b) White Space

Fig. 7. Link Capacity Per Channel v.s. Primary Interference, $d = 10m$, ITU-R P1411 Model, w/o IC, and $\sigma_s = \sigma_b = 7.02dB$

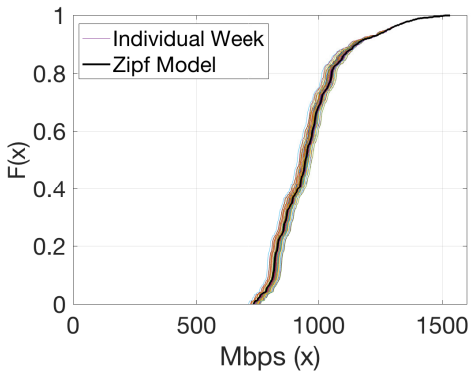

(a) CDFs of Capacity from Zipf model, and 46 weweekly rating instances 2011-2016

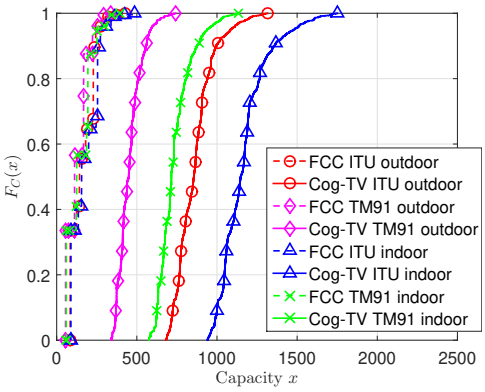

(b) Two Short-distance Path Loss Models, Outdoor and Indoor

Fig. 8. SHR Rank Vector in NYC for Evaluation.

decreases, the SU SINR on black-space channel increases until the limit set by power control, while on white space channel, it could keep increasing until the secondary interference became dominant. On both white and black space channels, the session capacity also increases by frequency due to frequency-induced path loss.

The CDFs of achievable capacity under Cog-TV framework in NYC generated from Zipf SHR and weekly SHRs of 46 weeks from 2011-2016 are illustrated in Fig. 8(a). The variation of top-rated channels (up to $\pm 34\%$) does not pose significant influence on the estimated capacity from Zipf SHR. This is because the spectrum availability and capacity is mostly determined by unpopular channels which is the case for most channels given the Zipf-distribution of SHR. This validated our capacity model under uncertainty of TV rating variation.

The capacity gain of Cog-TV over FCC rules also depend on propagation environments, as illustrated by the CDFs of achievable capacity in NYC with different path loss models in Fig 8(b). Indoor operation is benefited more than outdoors as walls could mitigate interference on both PU and SU. Similarly, operation in urban environments (ITU-R P1411) is benefited more than suburban environments (TM91), due to its higher path loss exponent.

The step-by-step results of city-wide analytical model (*macro model*) in [3] on an individual black-space channel, $b_j = 48$, in NYC are illustrated in Figs. 9. The CDF of TV signal strength in NYC, as shown in Fig. 9(a), is used to calculate the CDF of session capacity, as shown in Fig. 9(b). The CDF of SA shown in Fig. 9(c) is generated with (12) in [3]. The CDF of achievable capacity in NYC, as shown in Fig. 9(d), is then generated according to the

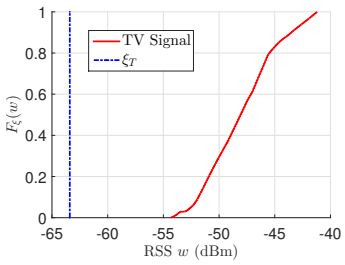

(a) TV Signal Strengh

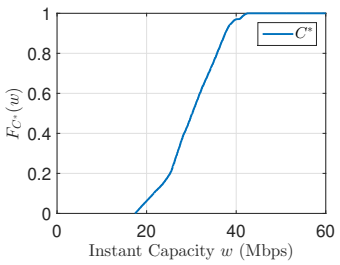

(b) Session Capacity

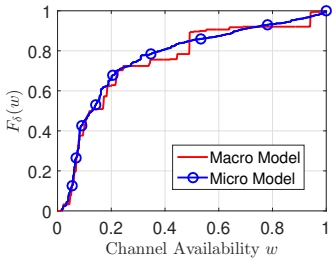

(c) Channel Availability

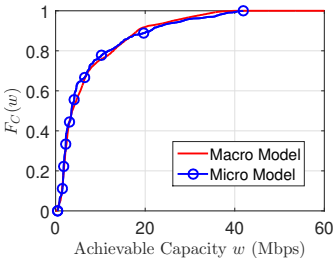

(d) Achievable Capacity

Fig. 9. CDFs of TV signal strength, Session Capacity, Spectrum Availability and Achievable Capacity on Channel 48, $k_y(48) = 13$, in NYC.

CDFs of session capacity and SA. For both SA and achievable capacity, the CDFs from *macro model* and the *micro model* are well matched, as shown in Figs. 9(c) and 9(d). This result validates the city-wide capacity model for individual black-space channel.

The spatio-temporal variation of spectrum availability in NYC

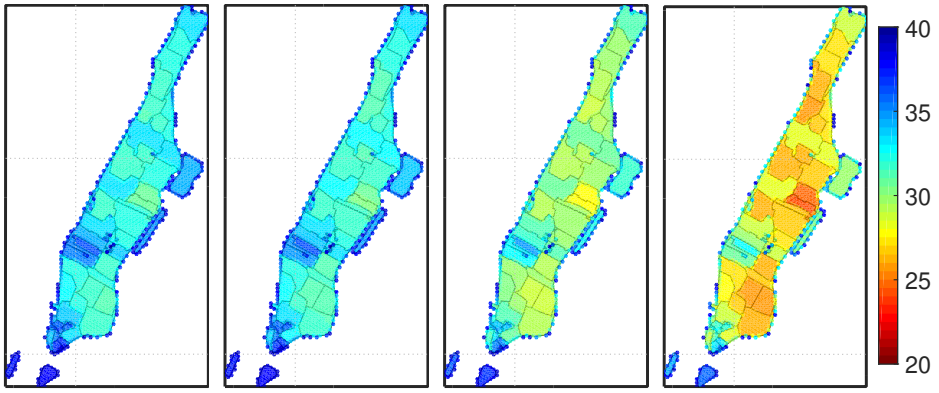

(a) 3:00 (b) 8:00 (c) 14:00 (d) 20:00

Fig. 10. Spatio-Temporal Distribution of Spectrum Availability in New York City in a Typical Day.

at different hours in a day based on the 24-hour pattern of household using Television (HUT) are illustrated in Fig. 10.

9 National Wide

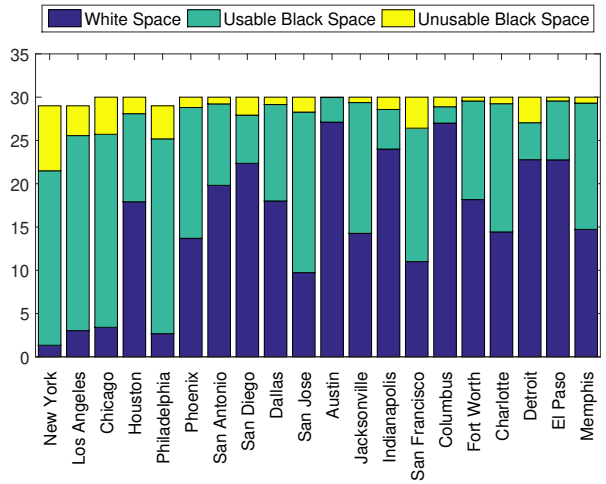

(a) Spectrum Availability

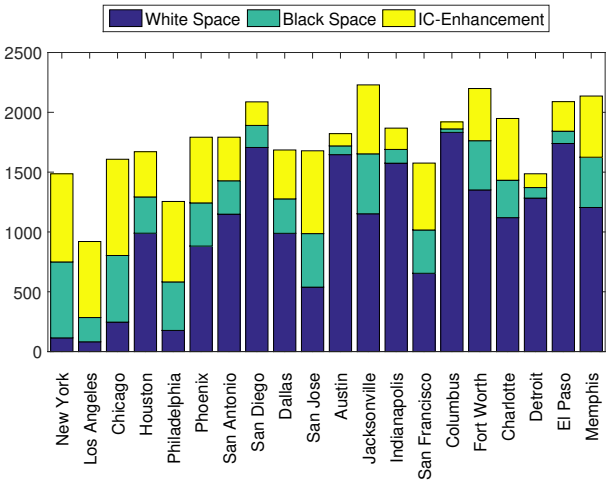

(b) Achievable Capacity, Outdoor

Fig. 11. Categorized Average Spectrum Availability and Achievable Capacity for Portable TVBDs under Cog-TV Framework in Top-20 U.S. Cities by Population

In Fig. 11, categorized Average Spectrum Availability and Achievable Capacity for Portable TVBDs under Cog-TV Framework in Top-20 US Cities are illustrated. It can observed in Fig. 11(a) that under Cog-TV framework, most part of the TV spectrum can be utilized in all these big cities. For those cities with limited TVWS, Cog-TV framework could enable the secondary TV spectrum access. From Fig. 11(b), it can be observed that because of the strong TV signals in some cities, such as Los Angles, the gain of Cog-TV framework without interference cancellaiton is very limited. However, with interference cancellation, the capacity of TV black-space can be improved on average 607 Mbps among the 20 cities.

10 Scalability of Cog-TV Framework

Scalability is one of the most important consideration of any spectrum sharing scheme. In the envisioned Cog-TV framework, primary users (e.g. TV sets) report their activities to a spectrum management system, and secondary users queries the spectrum management system and receive instructions for spectrum mobility. On the other hand, secondary users and/or primary users could also report their measurements of TV signals and/or performance metric (SINR) to the spectrum management system for better protection of TV viewers, for example, by control the SU transmit power. With regard to the scalability of such spectrum sharing system, two aspects are particularly considered:

The first and most important objective is obtaining the activities of TV sets to enable spectrum sharing. The most scalable approach is to embrace the next generation TV standard, ATSC 3.0, by which Cog-TV framework could be scaled up as this new standard. It would require the wireless network community to move towards this direction: collaborate with TV industry and regulatory body in various issues, including technical specifications, policy and privacy issues, and viable business models.

The second aspect is to design a scalable spectrum management system capable of real-time, interactive operation. New spectrum management infrastructure would be required to meet the stringent timing requirements of handling the TV zapping events and evacuating SUs as described in the paper. Zapping events reported by PUs and spectrum scheduling instructions issued to SUs are mainly over the backhaul networks, on which, the congestion could be mitigated by carefully engineering a real-time spectrum management infrastructure with proper population

coverage. On the SU side, feedback for spectrum sensing, e.g. TV signal strength, would only need to be sporadic to collect long term statistics. This is because the SU transmit power control model already takes fading margin in to consideration. Therefore, spectrum sensing activities could be scheduled by Cog-TV base-station or access point to avoid congesting the spectrum.

For the spectrum scheduling over the backhaul networks, the overall evacuation delay of a secondary user, t_E, can be modeled as the sum of network latency, t_N, response time of spectrum manager, t_D, and spectrum handover overhead, t_H, as shown in Fig. 12(a):

$$t_E = t_N + t_D + t_H \ . \tag{7}$$

Based on the statistics of network delay from Internet Service Providers [8], [9], [10], we consider the average round trip latency from coastal cities to Lincoln is 25 ms, and the average round trip latency within the same city as 3ms. The variance of network latency is $\sigma^2 = 0.907$.

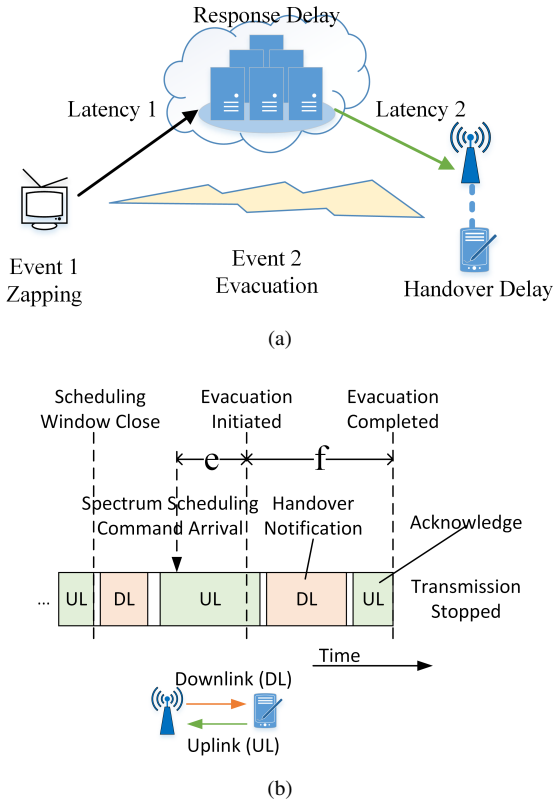

Fig. 12. (a) Physical Model, (b) Secondary User Delay.

The handover delay, as shown in Fig. 12(b), contains a delay of SU AP issuing instructions to SU mobile device, e, and the reaction time of the mobile device, f:

$$t_H = e + f \ , \tag{8}$$

The frame length of the communication protocol is assumed to be 20 ms, which is the maximum frame length of WiFi network. As a result, in this evaluation, the spectrum handover overhead of secondary link follows uniform distribution, $t_H \sim \mathcal{U}(20ms, 40ms)$.

The response time of a spectrum management job that involves searching relevant SUs from total N SUs for the PU, and searching relevant PUs out of M PUs that would be interfered by SUs, can be expressed as:

$$t_p = g(M+N) + gMn + hmn + l \ , \tag{9}$$

where g is the unit time consumption for searching an item in the database, h is the unit time of looking up channels occupied by a PU, m and n are the average relevant PUs and SUs, and l is a random delay caused by internal uncertainty of the computing system, such as scheduling delay of Operating System. The database response time is considered to be 6–50ms when the records in the database is equal to or less than 1 million. In [11], the average response time of a query in disk-based database for dataset size of 1,200, 4,800, and 19,000 is reported as 6, 26, and 220 milliseconds, respectively. For telecommunications, fast response is achieved by in-memory database [12], [13]. For example, IBM solidDB [14], can reduce the response time from 375 milliseconds in disk-based database to 50 milliseconds, and achieve an average of 1.2 million transactions per second for a dataset of 1 million records. In [12], SolidDB is reported to achieve 140,000 transactions per seconds on Flash-backed DRAM storage device.

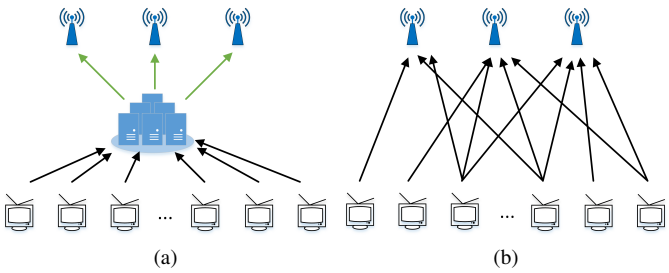

Fig. 13. Spectrum Management: (a) Centralized (b) Fully Distributed.

We evaluate 2 solutions based on assumed and collected parameters of aforementioned network latency model, frame length, and evacuation model. As shown in Figs. 13(a) and 13(b), the two solutions are:

- Fully distributed solution where each secondary access point handles the spectrum management functionality for itself. The number of processors of spectrum manager is set to 1.
- Regional Centralization, where a spectrum manager taking care of all the TV receivers in the city it located in. The number of processors in the spectrum manager is assumed to be 32.

The Over-The-Air TV ownership rate is set to 14%. A city of 8 million population (1.12 million Over-The-Air TV receivers) is considered for the regional spectrum manager case. The TV usage level is considered to vary from 5% to 60% from the middle night to prime time in a typical day. We assume that on average there are 10 to 200 secondary users in the guard zone (radius of 130 meters) of each primary user.

10.1 Fully Distribution

In the fully distributed scenario, the average network latency is 3ms. In this case, the number of registered TV receivers at each spectrum manager (in this case an individual secondary access point) is less than or equal to 130. This means that the relational database at the spectrum manager has at most a few hundred records. The response time of this tiny relational database will be fastest, 10 ms. Based on these conditions, we can find the average evacuation time for the fully distributed spectrum manager is 32 to 55 ms.

TABLE 1
Summary of Average Channel Evacuation Time of 2 Levels of Centralization

Centralization	No. of Processor	No. of TV Receivers	Network Latency	SM response time	Evacuation Time
Fully Distributed	1	≤ 130	2 ms	10 ms	35 to 55 ms
Regional Centralization	32	1.12 million	5 ms	120 ms	155 ms

10.2 Regional Centralization

In the regional centralization scenario, we assume that one spectrum manager located inside the city handles all the TV receivers in a city. In this setting, the number of TV receivers is assumed to be 1.12 million. The number of secondary users in the guard zone of TV receiver is 10-200. The spectrum manager is assumed to be a small workstation, which has 32 processors. We assume that the spectrum manager use in memory database which has the fastest response among all the database solutions. The response time of a single query is 6ms, and the response time average job will handle 200 records, with the probability of 0.1 for secondary users to evacuate the channel. Therefore, each job at the spectrum manager that will issue evacuation instruction will take about $120 = 6 \times 200 \times 0.1$ ms. The average evacuation time t_E is 155 ms in regional centralized spectrum manager.

Finally, the average evacuation time in the distributed and centralized solutions is summarized in Table 1. The preliminary calculation shows that a secure and centralized real-time spectrum management infrastructure based on off-the-shelf networking and database technologies could serve a large city or a million population while keeping the TV user experience of Zapping time acceptable. However, we admit that implementation of this spectrum management infrastructure would also depends on many other issues, such as cyber security and privacy policies, therefore is left for future work.

REFERENCES

[1] Z. Zhao, M. C. Vuran, D. Batur, and E. Ekici, "Ratings for spectrum: Impacts of TV viewership on TV whitespace," in *IEEE GLOBECOM 2014*, Dec 2014, pp. 941–947.

[2] D. Rempe, M. Snyder, A. Pracht, A. Schwarz, T. Nguyen, M. Vostrez, Z. Zhao, and M. C. Vuran, "A cognitive radio tv prototype for effective tv spectrum sharing," in *IEEE DySPAN*, Mar. 2017, pp. 117–118.

[3] Z. Zhao, M. C. Vuran, D. Batur, and E. Ekici, "Shades of white: Impacts of population dynamics and TV viewership on available TV spectrum," *IEEE Trans. on Vehicular Technology*, May 2018, submitted to.

[4] H. Bezabih and et.al, "Digital broadcasting: Increasing the available white space spectrum using TV receiver information," *IEEE Vehicular Technology Magazine*, vol. 7, no. 1, pp. 24–30, March 2012.

[5] M. Newman, "Power laws, Pareto distributions and Zipf's law," *Contemporary physics*, vol. 46, no. 5, pp. 323–351, 2005.

[6] V. M. Muggeo, "Estimating regression models with unknown breakpoints," *Statistics in medicine*, vol. 22, no. 19, pp. 3055–3071, 2003.

[7] W. Hoeffding and W. Hoeffding, "A combinatorial central limit theorem," *Ann. Math. Statist*, 1951.

[8] "Windstream's real-time network latency," Windstream Wholesale, retrived by Nov. 20th, 2017. [Online]. Available: http://www.windstreamwholesale.com/network-latency-tool/

[9] "Ip latency statistics," Verizon. [Online]. Available: http://www.verizonenterprise.com/about/network/latency/#latency

[10] "U.s. network latendy," AT&T. [Online]. Available: http://ipnetwork.bgtmo.ip.att.net/pws/network_delay.html

[11] S. Matalqa and S. Mustafa, "The effect of horizontal database table partitioning on query performance." *Int. Arab J. Inf. Technol.*, vol. 13, no. 1A, pp. 184–189, 2016.

[12] J. Jose, M. Banikazemi, W. Belluomini, C. Murthy, and D. K. Panda, "Metadata persistence using storage class memory: Experiences with flash-backed dram," in *Proceedings of the 1st Workshop on Interactions of NVM/FLASH with Operating Systems and Workloads*, ser. INFLOW '13. New York, NY, USA: ACM, 2013, pp. 3:1–3:7. [Online]. Available: http://doi.acm.org/10.1145/2527792.2527800

[13] H. Zhang, G. Chen, B. C. Ooi, K. L. Tan, and M. Zhang, "In-memory big data management and processing: A survey," *IEEE Transactions on Knowledge and Data Engineering*, vol. 27, no. 7, pp. 1920–1948, July 2015.

[14] J. Lindström, V. Raatikka, J. Ruuth, P. Soini, and K. Vakkila, "Ibm soliddb: In-memory database optimized for extreme speed and availability." *IEEE Data Eng. Bull.*, vol. 36, no. 2, pp. 14–20, 2013.